*5944–5953* *Nucleic Acids Research, 2007, Vol. 35, No. 17* *Published online 28 July 2007*
*doi:10.1093/nar/gkm641*

# Tissue-dependent paired expression of miRNAs

**Seungil Ro, Chanjae Park, David Young, Kenton M. Sanders and Wei Yan***

Department of Physiology and Cell Biology, University of Nevada School of Medicine, Reno, NV 89557, USA

Received May 21, 2007; Revised August 2, 2007; Accepted August 3, 2007

## ABSTRACT

**It is believed that depending on the thermodynamic stability of the 5′-strand and the 3′-strand in the stem-loop structure of a precursor microRNA (pre-miRNA), cells preferentially select the less stable one (called the miRNA or guide strand) and destroy the other one (called the miRNA* or passenger strand). However, our expression profiling analyses revealed that both strands could be co-accumulated as miRNA pairs in some tissues while being subjected to strand selection in other tissues. Our target prediction and validation assays demonstrated that both strands of a miRNA pair could target equal numbers of genes and that both were able to suppress the expression of their target genes. Our finding not only suggests that the numbers of miRNAs and their targets are much greater than what we previously thought, but also implies that novel mechanisms are involved in the tissue-dependent miRNA biogenesis and target selection process.**

## INTRODUCTION

A total of 4584 mature miRNAs have been registered in the miRBase (as of May, 2007) (1–3). These miRNAs were identified from various organisms including primates, rodents, birds, fish, worms, flies and viruses. Sequences of the majority of the miRNAs are highly conserved across species, suggesting that miRNAs are important regulators of molecular and cellular processes. miRNAs are believed to function as post-transcriptional suppressors through binding their target mRNAs through base pairing and subsequently inducing either translational repression or mRNA destabilization (4). Several studies have shown that miRNAs are involved in the regulation of various cellular processes including cell differentiation (5,6), proliferation (7,8) and apoptosis (9). Recent studies also provide evidence that miRNAs are directly linked to viral diseases (10), neuronal development (11) and tumorigenesis (12–14). These findings suggest that miRNAs are as important as transcriptional factors in the control of gene expression in higher eukaryotes.

miRNAs are transcribed as 100–1000 nucleotide (nt) primary miRNAs (pri-RNAs) by RNA polymerase II, and are modified just like mRNAs, including 5′ capping and 3′ poly(A) tailing (15–17). The miRNA-encoding portion in the pri-miRNA forms a hairpin, which is cleaved by the double-stranded RNA (dsRNA)-specific ribonuclease Drosha and its cofactor DiGeorge syndrome critical region 8 (DGCR8) (18). The cleaved hairpin is 60–70 nt long and is called a precursor miRNA (pre-miRNA) (19–22). The pre-miRNA is then transported by Ran-GTP and Exportin-5 (EXP5) to the cytoplasm (23–26). The pre-miRNA is further processed by a second RNase III complex, consisting of Dicer and the trans-activator RNA-binding protein (TRBP), which generates a miRNA duplex containing two mature miRNAs (5′- and 3′-strand miRNAs) each ~22 nt in length (27–31). It is currently believed that a miRNA-induced silencing complex (miRISC) selects either the 5′- or 3′-strand miRNA, depending on the relative stability of the termini in the pre-miRNA duplex. The strand with lower stability of base pairing in the 2nd–4th nucleotides at the 5′ end of the duplex (called miRNA or guide strand) preferentially binds the miRISC and thus becomes accumulated and functional, whereas the other one (called miRNA* or passenger strand) is degraded (18,32,33). This 'strand bias' theory was based upon analyses of the thermodynamic stability profiles of pre-miRNAs and mature miRNAs as well as small interfering RNAs (siRNA) (18,32,33). According to this model, only a small portion of miRNAs displaying similar thermodynamic stability in both the guide and passenger strands is expected to show co-accumulation (33), whereas the majority of miRNAs are highly asymmetric and thus are subjected to strand selection (32,33). However, during our analyses of miRNAs in the miRBase, we found that 234 out of 969 known human and mouse miRNAs were actually miRNA pairs (117 pairs). In addition, many 5′-strand miRNAs were found in one species, whereas its 3′-strand counterparts were present in another species. Since majority of the miRNAs are highly conserved among different species, these observations suggest that both strands are expressed and accumulated as miRNA pairs, but their selective or simultaneous accumulation may be tissue dependent.

To test this hypothesis, we first predicted the sister miRNAs for all 'unpaired' miRNAs using a miRNA

*To whom correspondence should be addressed. Tel: 775 784 7765; Fax: 775 784 6903; Email: wyan@medicine.nevada.edu

sequence determination rule that we deduced by analyzing the stem-loop structures of the pre-miRNAs for 117 known human and mouse miRNA pairs. We further validated the expression of these predicted sister miRNAs using semi-quantitative PCR and ribonuclease protection assays. We also predicted target genes for paired miRNAs and functionally validated six target genes for a sister pair mir-30e-5p and mir-30e-3p. Our data reveal that selective or co-accumulation of both strands of miRNAs is highly tissue dependent and both strands of a miRNA pair can functionally suppress the expression of their target genes.

## MATERIALS AND METHODS

### miRNA sequence analyses

All human and mouse miRNAs were collected from the miRBase (1–3). miRNA genes were located on each genome using the UCSC genomic browser (http://genome.ucsc.edu/) (34,35). A sequence containing a 100-bp upstream segment and a 100-bp downstream segment around the miRNA was used as a pre-miRNA to generate the secondary stem-loop structure using the MFOLD program version 3.2 (http://frontend.bioinfo.rpi.edu/applications/mfold/cgi-bin/rna-form1.cgi) (36,37). Most pre-miRNA sequences could fold into expected stem-loop structure as shown in the miRBase. For the ones that failed to fold into stem-loop structures initially, the flanking sequences were trimmed to get favorable folding. Both strands were then located in the stem-loop structures. Sizes of miRNAs, core sequences and overhangs were analyzed. The size distributions were calculated using Microsoft Excel (Office 2003, Microsoft). Data were plotted and graphed using GraphPad Prism (GraphPad Software).

By analyzing the commonality of the 5′- and the 3′-strand miRNA sequences in the duplex structures, we deduced a '3-Prime-Counting-22-nt' rule for the prediction of sister miRNAs based upon the known strands. Using this rule, we predicted sister strands for all currently known unpaired human and mouse miRNAs in the miRBase. To see whether the predicted sister miRNAs matched any of the known miRNAs or Piwi-interacting RNAs (piRNAs), all predicted miRNAs were searched for in the miRBase and in the GenBank at the NCBI website (http://www.ncbi.nlm.nih.gov/blast/).

### Small RNA isolation

Small RNA samples from 12 different mouse tissues (brain, heart, liver, spleen, lung, kidney, stomach, small intestine, colon, ovary, uterus and testis) were isolated using the mirVana$^{TM}$ miRNA isolation kit (Ambion) according to the manufacturer's instructions.

### Semi-quantitative RT-PCR analyses of miRNAs

Preparation of the small RNA complementary DNA (srcDNA) library and semi-quantitative PCR analyses of miRNAs were performed as described (38). All oligos used in this study are shown in the Supplementary Table 1. Semi-quantitative PCR analyses using srcDNAs were performed such that the PCR cycle numbers were empirically determined to ensure that each of the amplification reactions was in the exponential range (20–30 cycles). The house-keeping miRNA let-7d-5p (38) was used as a loading control.

### Ribonuclease protection assay (RPA)

For miRNA detection, RPA was performed using mirVana miRNA Probe Construction Kit (Ambion). For transcription of antisense RNA probes, DNA oligonucleotides (IDT) complementary to 5′-strand or 3′-strand of mir-24, mir-194 and mir-130a with the 12-nt linker sequence were synthesized (Supplementary Table 1). The 12-nt sequence is complementary to the T7 promoter primer provided in the kit. Each synthesized oligonucleotide (200 μM) was annealed with 2 μl of the T7 promoter primer in 6 μl of DNA hybridization buffer at 70°C for 5 min, followed by incubation at RT for 5 min. To get dsDNA template, end-filling reaction was performed by adding 2 μl of Klenow Reaction Buffer, 2 μl of 10 × dNTP Mix, 4 μl of Nuclease-free Water and 2 μl of Exo-Klenow at 37°C for 30 min. *In vitro* transcription was carried out to make RNA probes in a 20 μl reaction containing 1 μl of dsDNA template, 2 μl 10 × Transcription buffer, 1 μl of 10 mM ATP, 1 μl of 10 mM UTP, 1 μl of 10 mM CTP, 5 μl [α-$^{32}$P]GTP at 800 Ci/mmol and 10 mCi/ml (3.125 μM), 2 μl of T7 RNA Polymerase and 7 μl of Nuclease-free water at 37°C for 15 min, as described in the mirVana miRNA Probe Construction Kit Protocol (Ambion). After reaction, 1 μl of DNase I provided in the kit was added and incubated at 37°C for 10 min. The labeled RNA probes were purified using a purification filter cartridge provided in the mirVana Probe & Marker Kit (Ambion). Briefly, Binding/Washing Buffer (12 volumes of the sample) was added to the sample and mixed thoroughly. The mixture was applied to a purification filter cartridge and centrifuged. The cartridge was washed with 300 μl of Binding/Washing Buffer. The RNA probes were recovered with two sequential elutions using 20 μl of pre-heated (95°C) Elution Buffer each time. About 2 μg of small RNAs isolated from brain, heart, liver, spleen, lung and testis were used to hybridize with 1 μl each of the RNA probes, 10 μl of 2 × Hybridization Buffer, 2 μg of Yeast RNA at 42°C for 2 h using mirVana miRNA Detection Kit (Ambion). After hybridization, an aliquot of 150 μl of diluted RNase was added to digest free RNA probes and the samples were incubated at 37°C for 45 min. The digestion reaction was stopped by adding 225 μl of RNase Inactivation/PPT solution. Equal volumes (225 μl) of 100% ethanol were added to purify the probe-miRNA duplexes and the samples were stored at −20°C for 30 min. The samples were centrifuged at 12 000 r.p.m. for 10 min. The pellets were air-dried and resuspended in 15 μl of Gel Loading Buffer II. The samples were incubated at 95°C for 3 min and separated on a 15% denaturing polyacrylamide gel. The gel was photographed on the ChemiDoc XRS imaging system (Bio-Rad).

### miRNA target gene prediction and selection

Target genes for each of the sister strands were predicted and retrieved from the miRBase (http://microrna.sanger.ac.uk/) using the miRanda algorithm (3,39) with a *P*-value cutoff at 0.05 and also from the PicTar (http://pictar.bio.nyu.edu/) (40,41). The predicted targets for each sister strand were downloaded in the .txt format (the option is at the top of the page) and imported into Excel using the 'Data->Import External Data' option. Total target numbers for each sister strand were calculated and then average numbers for each sister strand were calculated using the Excel (Microsoft) and graphed using Prism (GraphPad Prism) (Figure 3). Target genes for the 5′-strand and the 3′-strand of mir-30e were predicted and analyzed using the miRBase Targets Version 4 (3). Based on scores and *P*-values, six potential target genes (*Akap14*, *Tshb*, *Sap30*, *Mrps30*, *Npffr2* and *Spata19*) were selected for experimental validation (Figure 4D).

### Construction of the miRNA-target validation vector

A miRNA-target validation vector was constructed from a luciferase reporter vector pGL4.19 [luc2CP/Neo] (Promega) and was named pGL-miTar (Supplementary Figure 7). SV40 promoter region (474 bp) was amplified with a primer pair containing the KpnI (forward) and HindIII (reverse) sites by PCR from the pGL4.19 (for primers, see Supplementary Table 1). The SV40 promoter was then inserted at the multiple cloning sites KpnI–HindIII before the luciferase gene (*Luc2*). An eGFP gene cassette (996 bp, eGFP- SV40 poly A signal) was amplified from the pAd Sh/H1 vector (42) and subcloned into pcDNA 3.1 TOPO vector. A chimeric intron (78 bp) with XmaI site in the middle used for adding the pre-miRNA sequences was inserted at the middle (335 bp from ATG) of the eGFP-coding region by mutagenesis PCR (eGFP-pre-miRNA/pDNA3.1) (for the chimeric intron sequence, see Supplementary Table 1). The eGFP-pre-miRNA cassette (2056 bp, CMV promoter-eGFPa-chimeric intron-eGFPb-SV40 poly A signal) was digested with BglII and XhoI and used to replace the neomycin gene cassette (1627 bp, BamHI–SalI) in the vector. The pGL-miTar was used for cloning a pre-miRNA and a target sequence into the chimeric intron and the 3′UTR of *Luc2*, respectively (Figure 4B). A mir-30e precursor (pre-mir-30e, 98 bp) with XmaI site at each end was amplified from the mouse genomic DNA and subcloned into pcDNA3.1 TOPO vector (Invitrogen) (for pre-mir-30e primers, see Supplementary Table 1). The pre-mir-30e was digested with XmaI from the plasmid isolated and subcloned into the pGL-miTar linearized with the same restriction enzyme. Target regions (120–186 bp) for each gene with XbaI site at each end were amplified from mouse testis cDNA and subcloned into the pcDNA3.1 TOPO vector (Invitrogen) (for each target gene primers, see Supplementary Table 1). Each target region was digested with XbaI and subcloned into the pGL-mir-30e linearized with the same restriction enzyme. The sequence accuracy and correct orientation of the pre-mir-30e and target region in the vector were confirmed by sequencing (for sequencing primers, see Supplementary Table 1). Bacteria transformed with each of the six final constructs were cultured in 500 ml LB medium and the plasmids were isolated using an endotoxin-free, EndoFree Plasmid Maxi Kit (QIAGEN).

### Dual-luciferase reporter assay

A Dual-Luciferase Reporter Assay System (Promega) was used to examine the effects of miRNAs on their target genes. Each mir-30e-target plasmid (2 μg) was co-transfected with pRL-CMV (10 ng) (Promega) into HEK-293 cells grown on a 6-well plate using PolyFect transfection reagent (20 μl) (QIAGEN). The transfected HEK cells were cultured for 24 h and used for the luciferase assay. The cells were washed with PBS buffer and homogenized with 200 μl of Passive Lysis Buffer. Luciferase Assay Buffer (100 μl) was transferred into a 96-well plate. The lysate (20 μl) was added into two wells (duplicate) of the 96-well plate and mixed. Firefly luciferase activity was measured on GloRunner Microplate Luminometer (Turner BioSystems). The plate was removed from the luminometer, Stop & Glo Reagent (100 μl) was added and mixed. The Renilla luciferase activity was measured on the luminometer. Data recorded on the luminometer were analyzed using Excel (Microsoft) and graphed using Prism (GraphPad Prism).

## RESULTS AND DISCUSSION

### Analysis of 117 pairs of mouse and human miRNAs in the miRbase

Among the 969 mouse and human miRNAs registered in the miRBase (as of May, 2007) (1–3), 377 (39%) are 5′-strand miRNAs and 358 (37%) are 3′-strand miRNAs. The remaining 234 are paired miRNAs (117 pairs) containing both the 5′-and 3′-strands (2) (Supplementary Table 2). Among these 234 paired miRNAs, 82 miRNAs (41 pairs) are from the mouse and 152 (76 pairs) are from the human. Interestingly, 114 (57 pairs) out of the 152 paired human miRNAs (76 pairs) registered in the miRBase (2) (highlighted in Supplementary Table 3) were previously shown to display a thermodynamic preference for the selection of either the 5′- or the 3′-strand (18). Moreover, we found an additional 32 pairs of miRNAs expressed as sister pairs in other species including the mouse (*Mus musculus*), cow (*Bos Taurus*), rat (*Rattus norvegicus*), chicken (*Gallus gallus*), zebra fish (*Danio rerio*), frog (*Xenopus tropicalis*) or fruit fly (*Drosophila melanogaster*) (highlighted in Supplementary Table 4). These 32 paired miRNAs were previously shown to be thermodynamically asymmetric (18). These findings suggest that the current 'thermodynamic stability' theory on strand selection is not universally followed during natural miRNA biogenesis. We hypothesized that in some tissues miRNAs were expressed and accumulated as sister pairs (5′- and 3′-strand miRNAs) while in other tissues the same miRNAs may be subjected to strand selection by an unknown mechanism.

To test our hypothesis, we need to develop a method to accurately predict the sister miRNAs for all unpaired miRNAs and test whether both strands of a miRNA pair

are indeed co-accumulated in some tissues. To deduce a sequence determination rule for predicting sister miRNA sequences based upon known unpaired miRNAs, we analyzed the stem-loop structures of pre-miRNAs for all 234 paired miRNAs previously identified from humans (Supplementary Table 3) and mice (Supplementary Table 5). The miRNA sequences in the stem-loop duplexes are almost identical between the mouse and human. A paired miRNA in a stem-loop shows a duplex structure, consisting of a core sequence, where the 5′-strand base pairs with the 3′-strand with an overhang at the 3′ end. The size of the majority of the paired miRNAs (225 out of 234 miRNAs analyzed, 96%) ranges from 20 to 24 nt in length (Supplementary Figure 1A). The overall size distribution between the two species is similar, although human miRNAs appear to be a bit longer than mouse miRNAs. Most of the paired miRNAs (201 miRNAs, 86%) range from 21 to 23 nt in length, among which the 22 nt size is the most frequently found (101 miRNAs, 43%). Overhang sizes are more variable, ranging from 0 to 5 nt (Supplementary Figure 1B) with the 2 nt overhang being the most common (85 miRNAs, 36%). Variation in total size and overhang size may be due to the current cloning strategy, which uses a primer containing two degenerate nucleotides at the 3′ end during cDNA synthesis (43).

### A '3-Prime-Counting-22-nt' rule for determining sister miRNA sequences

Analyses of the sizes of the core sequences and overhangs in the stem-loop structures of 234 paired mouse and human miRNAs registered in the miRBase allowed us to deduce a '3-Prime-Counting-22-nt' rule for the prediction of sister miRNA sequences (Supplementary Figure 2). The deduced duplex structure is consistent with the observation that the RNase III digests dsRNAs and pre-miRNAs (e.g. pre-mir-30) in a staggered manner, leaving a 2 nt overhang at the 3′ end (4) which serves as a substrate for Dicer to generate 22–24 nt products in a ruler-like fashion (44). To predict the sister strand for a known miRNA, one needs to first locate the first nucleotide (nt) of the known strand and then find its base-pairing nt (BN) on the to-be-predicted strand. A reference nt (RN) is further determined by locating the 1st–4th nt 3′ next to the BN, depending upon whether a gap or gaps are present in the known or the to-be-predicted strand (see Supplementary Figure 2 for step-by-step procedures). The RN will be the last nt of the 3′ end of the predicted sister miRNA strand. Thus, once the RN is determined, one can count 22 nt from the RN toward the 5′ direction and the 22 nt sequence is determined as the predicted sister miRNA.

To test whether our deduced sequence determination rule is universally followed during natural miRNA biogenesis, we predicted sister miRNAs for all currently known unpaired miRNAs of humans (Supplementary Table 4) and mice (Supplementary Table 7). A total of 735 new sister miRNAs (408 human and 327 mouse miRNAs) were predicted. We then compared the predicted miRNAs with homologous miRNAs found in several other species. Since the majority of the miRNAs are highly conserved across different species, those homologous miRNA pairs in species other than humans and mice would serve as a standard for us to evaluate the accuracy of our prediction. A total of 111 predicted sister miRNAs were found to have homologs in other species (Supplementary Tables 4 and 7). About 77% of the predicted miRNAs exactly matched the first nucleotide of actual miRNA sequences (Supplementary Table 6). A $\pm 2$-nt variation in the 5′ ends was observed in the remaining 23% of the predicted ones (26 sister miRNAs). The $\pm 2$-nt variation may be due to a gap or gaps in the duplex structures, which may be an important factor in determining the total size and overhang size of a mature miRNA. This notion is also supported by variations in the total size (20–24 nt) and overhang size (0–5 nt) shown in Supplementary Figure 1. Without considering gaps in either strand, only 53% of the predicted sister miRNAs showed 5′ends with a $< \pm 4$-nt error, as opposed to 100% with a $< \pm 2$-nt error if gaps were considered. The sequence match between the predicted 111 mouse and human sister miRNAs and their homologs in other species suggests that the '3-Prime-Counting-22-nt' rule is accurate in predicting the sequences for sister miRNAs.

### Validation and expression profiling of paired mouse miRNAs

We next randomly selected 47 paired mouse miRNAs, including 22 novel sister miRNAs predicted in this study, to validate their expression in mouse tissues. We had previously developed a PCR-based method for detection and quantification of miRNAs (38). This method is accurate, less time-consuming and much more sensitive than the traditional PAGE-based Northern blot analyses. We examined the expression levels of 47 paired miRNAs, including eight let-7 isoforms (let-7a to let-7i) in multiple mouse tissues using the semi-quantitative PCR in conjunction with ribonuclease protection assays (Figure 1). All of the 47 miRNAs were readily detected (Figures 1 and 2, Supplementary Figures 3–6) and each miRNA PCR product was sequenced to confirm their identity. As a representation, duplex structures and expression profiles of both strands of three miRNAs, mir-24, mir-194 and mir-130a are shown in Figure 1. Both strands of mir-24 have been previously identified from the mouse and human (Figure 1A). Only the 5′-strand of mir-194 and the 3′-strand of mir-130a were identified in both species, respectively. The 3′-strand of mir-194 (Figure 1D) and the 5′-strand of mir-130a (Figure 1G) were predicted using the '3-Prime-Counting-22-nt' rule. Both strands of mir-24, the 5′-strand of mir-194 and the 3′-strand of mir-130a displayed a ubiquitous expression pattern in all the tissues examined (Figure 1B, E and H). The 3′-strand of mir-194 and the 5′-strands of mir-130a, however, were preferentially expressed in some, but not all of the tissues tested (Figure 1E and H). For example, the 5′-strand of mir-130a is preferentially expressed in lung and uterus, but almost no expression was detected in liver, spleen, ovary and testis (Figure 1H and I). The ribonuclease protection assays (Figure 1C, F and I) showed that the expression patterns of the three miRNAs, mir-24, mir-194 and mir-130a were consistent with those of the PCR assays, further

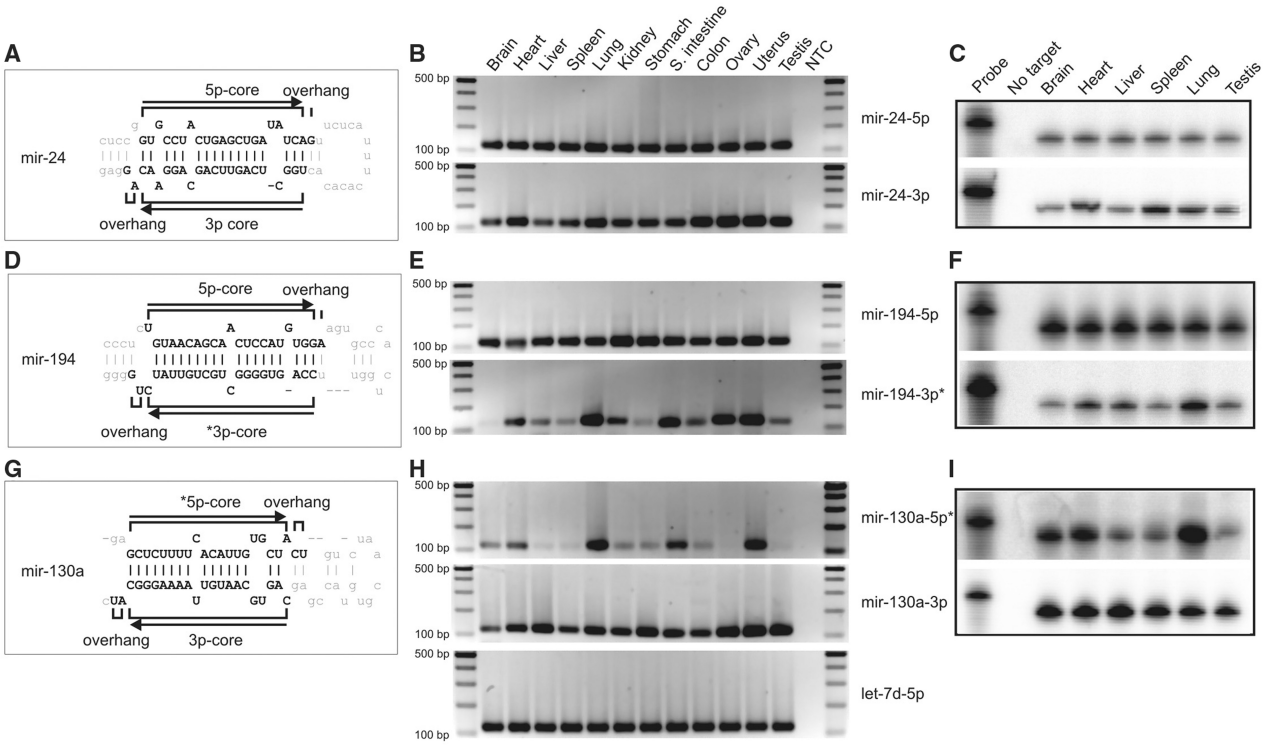


**Figure 1.** Duplex structures and expression profiles of the 5′-strand and the 3′-strand miRNAs of mir-24 (**A–C**), mir-194 (**D–F**) and mir-130a (**G–I**) in multiple mouse tissues. Both strands of mir-24 (mir-24-5p and -3p) were previously identified in the mouse and human. The 3′-strand of mir-194 (mir-194-3p) and the 5′-strand of mir-130a (mir-130a-5p) were predicted in this study and marked with asterisks (*). RNA sequences for each strand in the core used for designing PCR primers are indicated by arrows. Semi-quantitative PCRs were performed to examine levels of the 5′- and the 3′-strands of each miRNA (**B** for mir-24-5p and -3p, **E** for mir-194-5p and -3p and **H** for mir-130-5p and -3p) in 12 mouse tissues. The cycle numbers were empirically determined to ensure all amplification reactions were in the exponential range. A housekeeping miRNA let-7d-5p was used as a loading control. NTC stands for non-template negative control. A DNA ladder on each side indicates the size of the fragments. Detection of the 5′-strand and the 3′-strand miRNAs of mir-24 (C), mir-194 (F) and mir-130a (I) in six mouse tissues by ribonuclease protection assays are shown. Two controls, probe (probe without RNA sample and without RNase treatment), and no target (sample without RNA sample and with RNase treatment) for each miRNA were included.

indicating that our semi-quantitative PCR method is reliable.

It is unlikely that the detection of predicted sister strands resulted from the degenerating/degenerated miRNA* or passenger strands. The miRNA* or passenger strands not incorporated into the miRISC should be destroyed rapidly and thus not be accumulated in the tissues. In addition, levels of the miRNAs detected by the PCR represented their steady-state levels. Surprisingly, co-expression and co-accumulation of both strands of miRNAs are regulated in a tissue-dependent manner. Certain tissues express both strands as miRNA pairs [e.g. co-expression of both mir-194-5p and -3p in heart, lung, small intestine, ovary and uterus (Figure 1E and F)], whereas only single strands are accumulated in the other tissues [e.g. selective accumulation of mir-194-5p in brain, liver, spleen, stomach and testis (Figure 1E and F)]. This spatial regulation of miRNA expression and accumulation implicates that a novel tissue-dependent mechanism rather than the thermodynamic asymmetry is involved in the decision of selective or simultaneous accumulation of sister strands.

Consistent with the expression profiles of the three paired miRNAs (Figure 1), the other 36 paired miRNAs also displayed differential expression patterns in the multiple tissues. The eight let-7 isoforms are ubiquitously expressed in all tissues tested, but expression levels of each miRNA are different in different tissues (Figure 2A and Supplementary Figures 3 and 6). Among tissue-specific miRNAs observed, many miRNAs (mir-201-5p, mir-202-5p and 3p, mir-465-5p and 3p, mir-470-5p, mir-471-5p and 3p, mir-181b-1-3p) are preferentially expressed in the testis (Supplementary Figures 4C, 4D, 5A, 5C, 5D and Figure 2B). We further validated the expression of the other 60 paired miRNAs in the miRBase using the same semi-quantitative PCR method (Supplementary Tables 5 and 7, gel pictures available upon request) and found that early identified miRNAs (e.g. let-7s and mir-1 to 200) are mostly ubiquitously expressed in multiple mouse tissues, whereas the ones recently identified (e.g. mir-740s and mir-460s-470s) (45,46) or predicted sister miRNAs tend to be preferentially or tissue-specifically expressed. Since most of the early identified miRNAs are ubiquitously expressed, it is likely that their ubiquitous expression accounts for their early identification. Also, the finding that not all miRNAs are ubiquitously expressed may explain why many of our predictions, which may be preferentially expressed in only certain tissues, have not yet been cloned.

This finding also suggests that there may be many more tissue-specific miRNAs remaining to be identified.

### Expression profiling of paired miRNAs encoded by multi-copied genes

Some miRNA genes have multiple copies on the same chromosome or different chromosomes. It is unknown whether multiple copies are all transcribed, or whether only one is transcribed while the others act as pseudogenes and remain silent. We therefore attempted to examine the expression of the same miRNAs transcribed from two loci on different chromosomes. We analyzed three let-7 isoforms (let-7a, c and f), mir-181b and 194, which are all transcribed from two loci on different chromosomes (Figure 2 and Supplementary Figure 6). Sequences and chromosome locations are shown in Supplementary Table 8. let-7c-5p and two sister miRNAs were ubiquitously expressed in multiple mouse tissues (Figure 2A). The gene for mir-181b-5p has two copies, with one on chromosome 1 and the other on chromosome 2. Genomic sequences of the mir-181b-3p gene on chromosome 1 (named mir-181b-1-3p) and on chromosome 2 (named mir-181b-2-3p) are slightly different and thus can be distinguished using sequence-specific primers in the semi-quantitative PCR analyses (Supplementary Table 8). mir-181b-5p, mir-181b-2-3p and mir-194-1-5p are ubiquitously expressed in multiple mouse tissues, whereas mir-181b-1-3p, mir-194-1-3p and mir-194-2-3p are expressed in a tissue-preferential manner (Figure 2B for mir-181b, Supplementary Figure 6C for mir-194). These data suggest that all miRNAs analyzed in this study are indeed transcribed from two loci on different chromosomes. miRNAs encoded by genes with multiple copies have been assumed to be the same and thus grouped under the same miRNA identifiers. In the mouse and human, 161 miRNAs are derived from genes with at least two copies on the same or different chromosome(s). However, the sequence analysis of the sister miRNAs from different loci and the expression data that we show here demonstrate that sequences of sister miRNAs are different and that the expression patterns of each of them are unique. We therefore suggest that all the miRNAs derived from multiple copies of the same genes should be regarded as individual miRNAs.

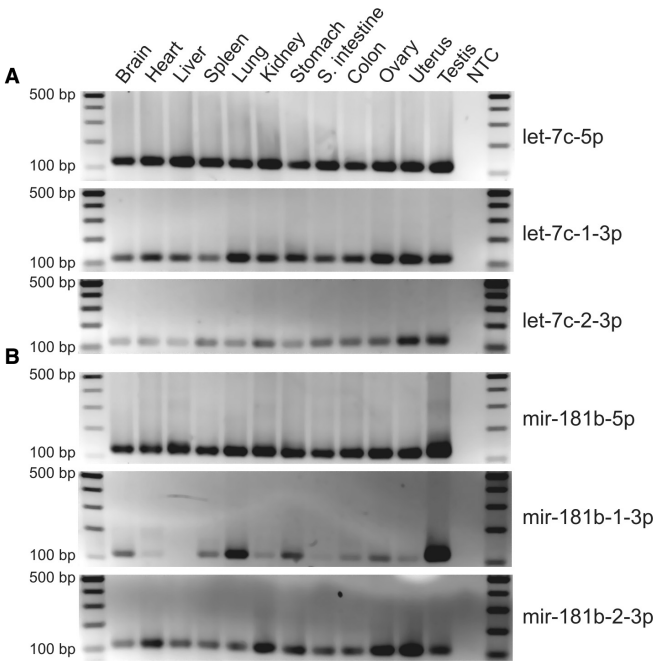


**Figure 2.** Expression profiles of miRNA pairs of let-7c and mir-181b transcribed from two loci on different chromosomes. Levels of the 5′- and the 3′-strands of each miRNA in 12 mouse tissues were analyzed using semi-quantitative RT-PCR with cycle numbers empirically determined to be within the exponential range. NTC stands for a non-template control. A DNA ladder on each side indicates the size of the fragments. A housekeeping miRNA let-7c-5p was used as a loading control. (**A**) Expression profiles of let-7c-5p and two sister 3′-strand miRNAs transcribed from two loci on chromosomes 16 and 15. Note: let-7c-5p transcribed from the two loci displays an identical sequence, whereas the two sister 3′-strand miRNAs transcribed from the two loci are slightly different in their sequences and thus can be distinguished using specific primers in the PCR assays (for sequences see Supplementary Table 8). (**B**) Expression profiles of mir-181b-5p and the two sister 3′-strand miRNAs transcribed from two loci on chromosomes 1 and 2. Note: mir-181b-5p transcribed from the two loci have an identical sequence, whereas two sister 3′-strand miRNAs derived from the two loci are different in their sequences and thus can be distinguished using specific primers in the PCR assays (for sequences see Supplementary Table 8).

### Similar numbers of target genes predicted for the 5′-strand and 3′-strand of a miRNA pair

The co-accumulation of both sister strands of a miRNA pair does not necessarily mean that both are functional, since one of the pair may target less, or even may not target any genes. To assess whether both sister miRNAs can target similar numbers of mRNAs, we analyzed the predicted target genes for 103 paired miRNAs (mouse 43 and human 60 pairs). The target genes predicted using the miRanda algorithm showed that both strands of paired miRNAs can target comparable average numbers of potential target genes in mice and humans (Figure 3). In mice, the average target numbers were 908.9 for the 5′-strand miRNAs and 899.0 for the 3′-strand miRNAs (Supplementary Table 9). Interestingly, human miRNAs

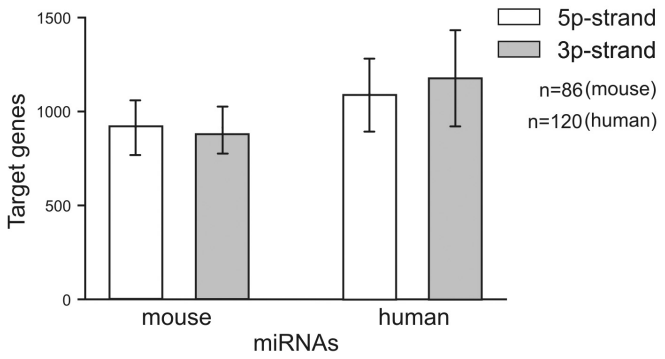


**Figure 3.** Average numbers of target genes predicted for paired miRNAs. Target genes for the 5′- or 3′-strands of paired miRNAs from mouse (86 miRNAs/43 pairs) and human (120 miRNAs/60 pairs) were predicted using the miRanda algorithm with a *P*-value cutoff at 0.05. Data were retrieved using the miRBase Targets Version 4 (Means ± SD, $n = 204$).

appear to have more predicted targets (1083.4 predicted targets for the 5′-strand miRNAs and 1166.5 for the 3′-strand miRNAs, Supplementary Table 10) than the mouse ones using the same algorithm although mice and humans are predicted to have the same number of protein-encoding genes (~30 000) in each genome (47,48). Forty-six out of the 59 human miRNA pairs analyzed here were previously thought to show a thermodynamic preference for the selection of either the 5′- (28 miRNAs) or the 3′-strand (18 miRNAs) (Supplementary Table 10) (18). However, similar average numbers of targets for the 5′- and 3′-strands were predicted, respectively. The average number of target genes for the 28 5′-strand miRNAs were 1119.0 and that for their 3′-strand sister miRNAs was 1217.5. Likewise, the average number for the 18 3′-strand miRNAs were 1014.6 and that for their 3′-strand sister miRNAs was 1154.9. Using another popular target prediction program the PicTar (http://pictar.bio.nyu.edu/) (40,41), we predicted and analyzed the potential targets for each strand of the 40 paired miRNAs (mouse 27 pairs and human 13 pairs) available in this website. The average target numbers predicted by the PicTar algorithm (e.g. 188 for the 5′-strand and 174 for the 3′-strand of mouse paired miRNAs) were less than those predicted by the miRBase (909 for the 5′ strand and 809 for the 3′ strand in mouse paired miRNAs). However, average numbers of targets predicted for each strand of the 40 paired miRNAs appeared to be similar (Supplementary Tables 9 and 10), which is consistent with the target prediction results using the miRanda algorithm. These data suggest that both strands be equally functional.

### Both sister strands of a miRNA pair are functional

To test whether both sister strands of a miRNA pair can functionally suppress their target gene expression, we developed a miRNA-target validation system using a dual-Luciferase reporter assay. Using this system, we examined functionality of both strands of mir-30e (mir-30e-5p and mir-30e-3p). The paired miRNAs mir-30e-5p and -3p were chosen because they were previously shown to display differential thermodynamic stability, implicating that only the guide strand, corresponding to mir-30e-3p here, could be selectively accumulated and be functional (18). mir-30e-5p was cloned from the mouse embryonic stem cell (49), whereas mir-30e-3p was cloned from the human HL-60 cells (50). Interestingly, our semi-quantitative RT-PCR analyses revealed that both mir-30e-5p and mir-30e-3p were differentially expressed in most of the mouse tissues (Figure 4A). Consistent with the expression patterns of other miRNA pairs analyzed in this study, each strand showed a tissue-dependent expression: mir-30e-3p appeared to be preferentially accumulated in stomach, whereas mir-30e-5p was selectively accumulated in spleen (Figure 4A). Among numerous predicted target genes, three for mir-30e-5p (*Akap14*, *Tshb* and *Sap30*) and three for mir-30e-5p (*Mrps30*, *Npffr2* and *Spata19*) were chosen because they showed higher scores with lower *P*-values (Supplementary Table 11). For target validation, we constructed a miRNA-target validation vector pGL-miTar (Figure 4B). The target region for each of six genes

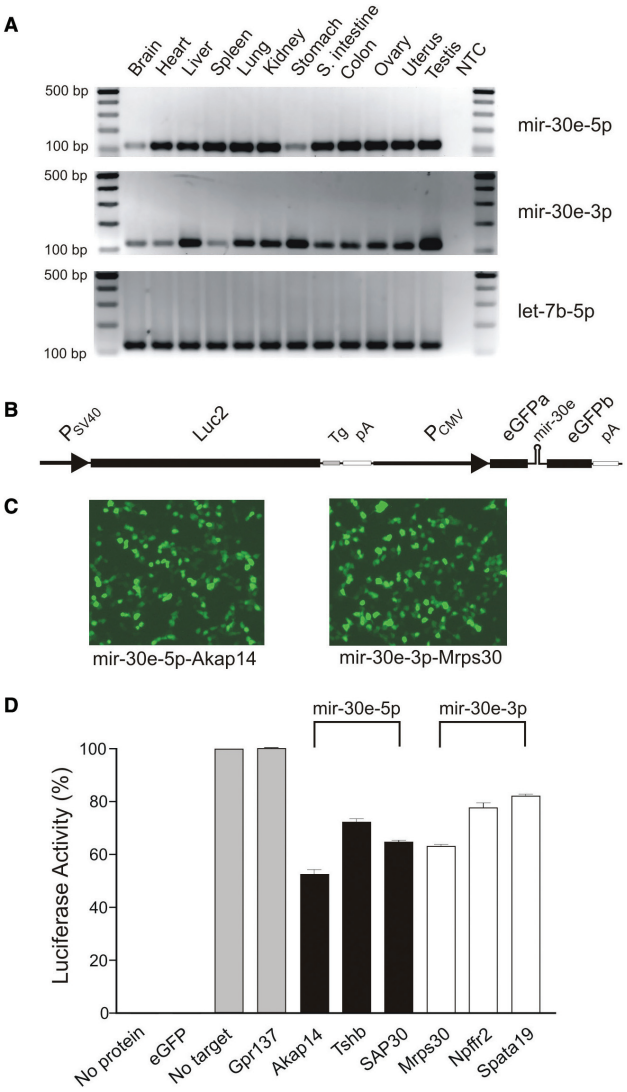


**Figure 4.** Suppression of target gene expression by a miRNA pair mir-30e-5p and mir-30e-3p. (**A**) Steady-state expression levels of mir-30e-5p and mir-30e-3p in 12 mouse tissues determined by semi-quantitative RT-PCR analyses. NTC stands for a non-template control. A DNA ladder on each side indicates the size of the fragments. A housekeeping miRNA let-7d-5p was used as a loading control. (**B**) A schematic map of the mir-30e-target validation vector. The pre-mir-30e (98 bp) with a chimeric intron was inserted in the middle of the eGFP-coding region (eGFPa and eGFPb). Each of the target-binding regions from the six predicted target genes (*Akap14*, *Tshb*, *Sap30*, *Mrps30*, *Npffr2* and *Spata19*) was inserted into the 3′UTR of the Luciferase gene (*Luc2*). $P_{SV40}$, SV40 promoter; Tg, target region; pA, poly (A) signal; $P_{CMV}$, CMV promoter. (**C**) GFP-positive HEK-293 cells transfected with mir-30e-5p-*Akap14* (left) and mir-30e-3p-*Mrps30* (right). Transfected cells were cultured for 24 h before visualization and photography under a fluorescent microscope. (**D**) Suppression of luciferase activity by interactions between the sister miRNA pair mir-30e-5p and mir-30e-3p and their corresponding targeting sequences at the 3′UTR of *Luc2*. Luciferase activities (Firefly luciferase and Renilla luciferase) in the cells co-transfected with each of the six target validation plasmids and pRL-CMV were measured. As negative controls, pGL-mir-30eTar (containing no target sequences) and pGL-mir-30e-*Gpr137* (containing a let-7d-5p target sequence) were used. The no-protein controls represent samples added with the buffer only and the eGFP controls were those transfected with the eGFP-expressing vector eGFP-pre-miRNA/pDNA3.1 only. The firefly luciferase activity was normalized against the Renilla luciferase. Reduction of the luciferase activity was presented as percentage of levels in the no target samples (Means ± SEM, $n = 3$).

(120–186 bp) was amplified from the mouse testis cDNA and then subcloned into the 3′UTR of the Luciferase gene (*Luc2*) (Figure 4B). The mir-30e precursor (98 bp) amplified from the mouse genomic DNA was inserted into the chimeric intron (36 bp 5′ donor and 36 bp 3′ acceptor sequences) of an *eGFP* gene so that the pre-mir-30e could be spliced from the eGFP transcript to produce the mir-30e sister pair. The remaining eGFP transcript would be spliced, ligated and translated into eGFP, which serves as a marker for monitoring not only transfection efficiency but also correct splicing. Two representative fluorescent images (Figure 4C) show that HEK-293 cells transfected with either the mir-30e-5p-*Akap14* vector or the mir-30e-3p-*Mrps30* construct expressed abundant eGFP. HEK-293 cells transfected with each of the other four miRNA-target validation constructs also expressed abundant eGFP (data not shown), indicating that the transfection was effective and the pre-mir-30e were correctly spliced. The pre-mir-30e processed by the Dicer of the cells should generate mature mir-30e-5p and mir-30e-3p, which would then be incorporated into the miRISC. The mir-30e-RISCs would bind their respective target sequences inserted at the 3′UTR of the *Luc2* gene and thus suppress levels of Luciferase in the assays. Luciferase activity was reduced by 18–48% in the cells transfected by each of the six miRNA-target sequence validation constructs (Figure 4D). Among the six target genes, *Akap14* showed the greatest reduction (48%) by mir-30e-5p, whereas *Spata19* displayed the least suppression (18%) by mir-30e-3p. As control experiments, we used pGL-mir-30eTar (contains no target sequences in the 3′UTR of the *Luc2*), or pGL-mir-30e-*Gpr137*, which contains the target sequence from the 3′UTR of *Gpr137*. *Gpr137* was predicted to be targeted by let-7d-5p, but not by either strand of mir-30e. As expected, no reduction in luciferase activity was observed in the cells transfected with pGL-30eTar (no target control) or pGL-mir-30e-*Gpr137*. These results suggest that both sister strands of the mir-30e are functional despite their varying efficiency in suppressing their target gene expression.

### A novel 'Target-Two-Sets-of-Genes-With-One-Pre-miRNA' model for miRNA biogenesis and gene silencing

The tissue-dependent co-accumulation of sister miRNAs is physiologically significant because it reveals, for the first time, that one pre-miRNA can produce two functional sister miRNAs which can target two sets of totally different genes. Based on our finding, we propose a 'Target-Two-Sets-of-Genes-With-One-Pre-miRNA' model, in which cells from certain tissues can utilize both strands of a sister miRNA pair rather than adopting one strand and discarding the other (Figure 5). Recent computational identification of target genes of miRNAs show that 148 human miRNAs can potentially target up to 5300 human genes, representing up to 30% of the gene set in the analysis (17 850 orthologous mammalian genes) (51). Human tissues express at least 968 miRNAs including 408 miRNAs predicted in this study, suggesting that miRNAs theoretically could target the entire mRNA transcriptome and that all the human mRNA-coding genes are under the regulation of miRNAs.

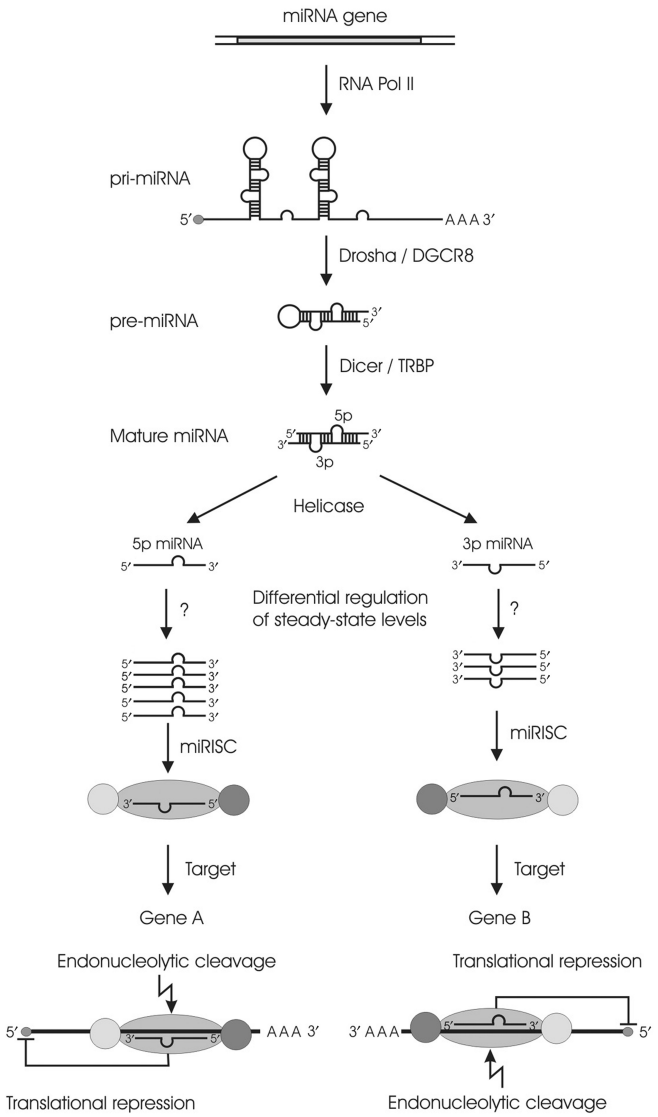


**Figure 5.** A new 'Target-Two-Sets-of-Genes-With-One-Pre-miRNA' model for miRNA biogenesis and target selection. In this model, a miRNA gene is transcribed by RNA polymerase II and is modified in the nucleus into a pri-miRNA, which is further processed to produce an ~60–70 nt pre-miRNA by the RNase III endonuclease Drosha and DGCR8. The pre-miRNA is then exported to the cytoplasm by Ran-GTP and Exportin-5. A 22-nt miRNA duplex is cleaved from the pre-miRNA by the second RNase III endonuclease complex including Dicer and TRBP. This mature miRNA duplex contains a 5′-strand (5p) miRNA and a sister 3′-strand (3p) miRNA, which is unwound by Helicase. Steady-state levels of each of the miRNA pair are independently regulated by an unknown tissue-specific mechanism. Each strand of the sister miRNA pair can be incorporated into miRISC to become an active miRNA. Since sister miRNAs bound to miRISC possess different sequences, they may target different portions of the same genes or completely different sets of genes to mediate the degradation or translational inhibition of their target mRNAs.

The differential expression levels of each strand suggest that the steady-state levels of each miRNA are independently regulated in different tissues. It is unlikely that the variation in the steady-state levels of a miRNA strand is

due to differential levels in nuclease activity since miRNAs that show similar steady-state levels in one tissue can display significantly different steady-state levels in another tissue, although within a given tissue the nuclease activity should be the same. For example, mir-20b-5p and mir-127-5p display comparable steady-state levels in brain, whereas the levels of mir-20b-5p are much higher than mir-127-5p levels in heart, liver and spleen (see frames in Supplementary Figure 4A and B). Furthermore, since the steady-state levels of a given miRNA can vary dramatically across different tissues, it is unlikely that the regulatory signal is contained entirely in the sequence or the thermodynamic stability of the miRNA. A plausible explanation is that some tissues may need both strands to regulate expression of the target genes. In other tissues, the target genes for one strand of a miRNA pair may not be expressed and the corresponding sister miRNA strand, therefore, may not be required. In this case, the sister miRNA should be subjected to degradation, which leads to the 'strand bias' phenomenon in these tissues. It is also possible that thermodynamic asymmetry plays a role in the differential expression of certain miRNAs across tissues, but that in some tissues an unknown mechanism rescues the accumulation of the more thermodynamically stable strand. Nevertheless, thermodynamic asymmetry is not the determining factor in miRNA expression and accumulation.

To be functional, each strand of a miRNA pair needs to be incorporated into the miRISC. It is very difficult to show experimentally the incorporation of all sister miRNAs into miRISC, and only a handful of miRNAs have been experimentally verified to be incorporated into RISC (33,52,53), in which artificial target constructs and siRNAs instead of miRNAs were used. In siRNAs, asymmetric siRNAs have been shown to result in asymmetric assembly of siRNA RISC (siRISC) (32,33). Although it was generally accepted that siRISC and miRISC are functionally interchangeable, recent data show that siRISC and miRISC are distinct complexes that regulate mRNA stability and translation in different interacting modes (54). The terminology of miRNA and miRNA* or guide and passenger strands that is used is based upon differences in the thermodynamic stability of the 5′ and the 3′ strands. However, our data suggest that thermodynamic stability apparently is not an exclusively determining factor for the selective accumulation or co-accumulation of both strands of miRNAs. Naming each strand of a paired miRNA according to its strand origin (e.g. mir-30e-5p and mir-30e-3p) will be more accurate and less confusing.

Taken together, our data demonstrated that mature functional miRNAs can be derived from either the 5′-strand, or the 3′-strand, or from both strands of the pre-miRNAs depending upon the tissues where they are expressed. Steady-state levels of each strand of a miRNA pair are differentially regulated across tissues or even in the same tissues. The '3-Prime-Counting-22-nt' sequence determination rule can be used for the prediction of sister miRNAs for the remaining ~3000 unpaired miRNAs from various organisms. Our findings demand further studies on the mechanisms underlying the dynamic regulation of tissue-dependent miRNA biogenesis and target selection.

## SUPPLEMENTARY DATA

Supplementary data are available at NAR Online.

## ACKNOWLEDGEMENTS

The Nevada Genomic Center is acknowledged for sequencing assays. This work was supported by grants from the National Institute of Health (HD048855), and a start-up fund from the University of Nevada, Reno, to W.Y. Funding to pay the Open Access publication charges for the article was provided by the University of Nevada, Reno.

*Conflict of interest statement*. None declared.

## REFERENCES

1. Ambros,V., Bartel,B., Bartel,D.P., Burge,C.B., Carrington,J.C., Chen,X.M., Dreyfuss,G., Eddy,S.R., Griffiths-Jones,S. *et al.* (2003) A uniform system for microRNA annotation. *RNA*, **9**, 277–279.
2. Griffiths-Jones,S. (2004) The microRNA Registry. *Nucleic Acids Res.*, **32**, D109–D111.
3. Griffiths-Jones,S., Grocock,R.J., van Dongen,S., Bateman,A. and Enright,A.J. (2006) miRBase: microRNA sequences, targets and gene nomenclature. *Nucleic Acids Res.*, **34**, D140–D144.
4. Kim,V.N. (2005) MicroRNA biogenesis: coordinated cropping and dicing. *Nat. Rev. Mol. Cell Biol.*, **6**, 376–385.
5. Chen,X.M. (2004) A microRNA as a translational repressor of APETALA2 in Arabidopsis flower development. *Science*, **303**, 2022–2025.
6. Dostie,J.E., Mourelatos,Z., Yang,M., Sharma,A. and Dreyfuss,G. (2003) Numerous microRNPs in neuronal cells containing novel microRNAs. *RNA*, **9**, 180–186.
7. Brennecke,J., Hipfner,D.R., Stark,A., Russell,R.B. and Cohen,S.M. (2003) Bantam encodes a developmentally regulated microRNA that controls cell proliferation and regulates the proapoptotic gene hid in Drosophila. *Cell*, **113**, 25–36.
8. Reinhart,B.J., Slack,F.J., Basson,M., Pasquinelli,A.E., Bettinger,J.C., Rougvie,A.E., Horvitz,H.R. and Ruvkun,G. (2000) The 21-nucleotide let-7 RNA regulates developmental timing in Caenorhabditis elegans. *Nature*, **403**, 901–906.
9. Xu,P.Z., Vernooy,S.Y., Guo,M. and Hay,B.A. (2003) The Drosophila MicroRNA mir-14 suppresses cell death and is required for normal fat metabolism. *Curr. Biol.*, **13**, 790–795.
10. Pfeffer,S., Zavolan,M., Grasser,F.A., Chien,M.C., Russo,J.J., Ju,J.Y., John,B., Enright,A.J., Marks,D. *et al.* (2004) Identification of virus-encoded microRNAs. *Science*, **304**, 734–736.
11. Krichevsky,A.M., King,K.S., Donahue,C.P., Khrapko,K. and Kosik,K.S. (2003) A microRNA array reveals extensive regulation of microRNAs during brain development. *RNA*, **9**, 1274–1281.
12. Calin,G.A., Sevignani,C., Dan Dumitru,C., Hyslop,T., Noch,E., Yendamuri,S., Shimizu,M., Rattan,S., Bullrich,F. *et al.* (2004) Human microRNA genes are frequently located at fragile sites and genomic regions involved in cancers. *Proc. Natl Acad. Sci. USA.*, **101**, 2999–3004.
13. Metzler,M., Wilda,M., Busch,K., Viehmann,S. and Borkhardt,A. (2004) High expression of precursor microRNA-155/BIC RNA in children with Burkitt lymphoma. *Genes Chromosomes Cancer*, **39**, 167–169.
14. Michael,M.Z., O'Connor,S.M., Pellekaan,N.G.V., Young,G.P. and James,R.J. (2003) Reduced accumulation of specific microRNAs in colorectal neoplasia. *Mol. Cancer Res.*, **1**, 882–891.
15. Cai,X.Z., Hagedorn,C.H. and Cullen,B.R. (2004) Human microRNAs are processed from capped, polyadenylated transcripts that can also function as mRNAs. *RNA*, **10**, 1957–1966.

16. Lee,Y., Kim,M., Han,J.J., Yeom,K.H., Lee,S., Baek,S.H. and Kim,V.N. (2004) MicroRNA genes are transcribed by RNA polymerase II. *EMBO J.*, **23**, 4051–4060.
17. Smalheiser,N.R. (2003) EST analyses predict the existence of a population of chimeric microRNA precursor-mRNA transcripts expressed in normal human and mouse tissues. *Genome Biol.*, 4:430.
18. Han,J.J., Lee,Y., Yeom,K.H., Nam,J.W., Heo,I., Rhee,J.K., Sohn,S.Y., Cho,Y.J., Zhang,B.T. *et al.* (2006) Molecular basis for the recognition of primary microRNAs by the Drosha-DGCR8 complex. *Cell*, **125**, 887–901.
19. Denli,A.M., Tops,B.B.J., Plasterk,R.H.A., Ketting,R.F. and Hannon,G.J. (2004) Processing of primary microRNAs by the Microprocessor complex. *Nature*, **432**, 231–235.
20. Han,J.J., Lee,Y., Yeom,K.H., Kim,Y.K., Jin,H. and Kim,V.N. (2004) The Drosha-DGCR8 complex in primary microRNA processing. *Genes Dev.*, **18**, 3016–3027.
21. Landthaler,M., Yalcin,A. and Tuschl,T. (2004) The human DiGeorge syndrome critical region gene 8 and its D-melanogaster homolog are required for miRNA biogenesis. *Curr. Biol.*, **14**, 2162–2167.
22. Lee,Y., Ahn,C., Han,J.J., Choi,H., Kim,J., Yim,J., Lee,J., Provost,P., Radmark,O. *et al.* (2003) The nuclear RNase III Drosha initiates microRNA processing. *Nature*, **425**, 415–419.
23. Bohnsack,M.T., Czaplinski,K. and Gorlich,D. (2004) Exportin 5 is a RanGTP-dependent dsRNA-binding protein that mediates nuclear export of pre-miRNAs. *RNA*, **10**, 185–191.
24. Lund,E., Guttinger,S., Calado,A., Dahlberg,J.E. and Kutay,U. (2004) Nuclear export of microRNA precursors. *Science*, **303**, 95–98.
25. Yi,R., Qin,Y., Macara,I.G. and Cullen,B.R. (2003) Exportin-5 mediates the nuclear export of pre-microRNAs and short hairpin RNAs. *Genes Dev.*, **17**, 3011–3016.
26. Zeng,Y. and Cullen,B.R. (2004) Structural requirements for pre-microRNA binding and nuclear export by Exportin 5. *Nucleic Acids Res.*, **32**, 4776–4785.
27. Bernstein,E., Caudy,A.A., Hammond,S.M. and Hannon,G.J. (2001) Role for a bidentate ribonuclease in the initiation step of RNA interference. *Nature*, **409**, 363–366.
28. Chendrimada,T.P., Gregory,R.I., Kumaraswamy,E., Norman,J., Cooch,N., Nishikura,K. and Shiekhattar,R. (2005) TRBP recruits the Dicer complex to Ago2 for microRNA processing and gene silencing. *Nature*, **436**, 740–744.
29. Grishok,A., Pasquinelli,A.E., Conte,D., Li,N., Parrish,S., Ha,I., Baillie,D.L., Fire,A., Ruvkun,G. *et al.* (2001) Genes and mechanisms related to RNA interference regulate expression of the small temporal RNAs that control C-elegans developmental timing. *Cell*, **106**, 23–34.
30. Hutvagner,G., McLachlan,J., Pasquinelli,A.E., Balint,E., Tuschl,T. and Zamore,P.D. (2001) A cellular function for the RNA-interference enzyme Dicer in the maturation of the let-7 small temporal RNA. *Science*, **293**, 834–838.
31. Ketting,R.F., Fischer,S.E.J., Bernstein,E., Sijen,T., Hannon,G.J. and Plasterk,R.H.A. (2001) Dicer functions in RNA interference and in synthesis of small RNA involved in developmental timing in C-elegans. *Genes Dev.*, **15**, 2654–2659.
32. Khvorova,A., Reynolds,A. and Jayasena,S.D. (2003) Functional siRNAs and rniRNAs exhibit strand bias. *Cell*, **115**, 209–216.
33. Schwarz,D.S., Hutvagner,G., Du,T., Xu,Z.S., Aronin,N. and Zamore,P.D. (2003) Asymmetry in the assembly of the RNAi enzyme complex. *Cell*, **115**, 199–208.
34. Kent,W.J., Sugnet,C.W., Furey,T.S., Roskin,K.M., Pringle,T.H., Zahler,A.M. and Haussler,D. (2002) The human genome browser at UCSC. *Genome Res.*, **12**, 996–1006.
35. Karolchik,D., Baertsch,R., Diekhans,M., Furey,T.S., Hinrichs,A., Lu,Y.T., Roskin,K.M., Schwartz,M., Sugnet,C.W. *et al.* (2003) The UCSC Genome Browser Database. *Nucleic Acids Res.*, **31**, 51–54.
36. Mathews,D.H., Sabina,J., Zuker,M. and Turner,D.H. (1999) Expanded sequence dependence of thermodynamic parameters improves prediction of RNA secondary structure. *J. Mol. Biol.*, **288**, 911–940.
37. Zuker,M. (2003) Mfold web server for nucleic acid folding and hybridization prediction. *Nucleic Acids Res.*, **31**, 3406–3415.
38. Ro,S., Park,C., Jin,J.L., Sanders,K.M. and Yan,W. (2006) A PCR-based method for detection and quantification of small RNAs. *Biochem. Biophys. Res. Commun.*, **351**, 756–763.
39. John,B., Enright,A.J., Aravin,A., Tuschl,T., Sander,C. and Marks,D.S. (2004) Human MicroRNA targets. *PLoS Biol.*, **2**, 1862–1879.
40. Chen,K. and Rajewsky,N. (2006) Natural selection on human microRNA binding sites inferred from SNP data. *Nat. Genet.*, **38**, 1452–1456.
41. Krek,A., Grun,D., Poy,M.N., Wolf,R., Rosenberg,L., Epstein,E.J., MacMenamin,P., da Piedade,I., Gunsalus,K.C. *et al.* (2005) Combinatorial microRNA target predictions. *Nat. Genet.*, **37**, 495–500.
42. Ro,S., Hwang,S.J., Ordog,T. and Sanders,K.M. (2005) Adenovirus-based short hairpin RNA vectors containing an EGFP marker and mouse U6, human H1, or human U6 promoter. *Biotechniques*, **38**, 625–627.
43. Fu,H.J., Tie,Y., Xu,C.W., Zhang,Z.Y., Zhu,J., Shi,Y.X., Jiang,H., Sun,Z.X. and Zheng,X.F. (2005) Identification of human fetal liver miRNAs by a novel method. *FEBS Lett.*, **579**, 3849–3854.
44. Vermeulen,A., Behlen,L., Reynolds,A., Wolfson,A., Marshall,W.S., Karpilow,J. and Khvorova,A. (2005) The contributions of dsRNA structure to Dicer specificity and efficiency. *RNA*, **11**, 674–682.
45. Watanabe,T., Takeda,A., Tsukiyama,T., Mise,K., Okuno,T., Sasaki,H., Minami,N. and Imai,H. (2006) Identification and characterization of two novel classes of small RNAs in the mouse germline: retrotransposon-derived siRNAs in oocytes and germline small RNAs in testes. *Genes Dev.*, **20**, 1732–1743.
46. Yu,Z.R., Raabe,T. and Hecht,N.B. (2005) MicroRNA Mirn122a reduces expression of the posttranscriptionally regulated germ cell transition protein 2 (Tnp2) messenger RNA (mRNA) by mRNA cleavage. *Biol. Reprod.*, **73**, 427–433.
47. Lander,E.S., Linton,L.M., Birren,B., Nusbaum,C., Zody,M.C., Baldwin,J., Devon,K., Dewar,K., Doyle,M. *et al.* (2001) Initial sequencing and analysis of the human genome. *Nature*, **409**, 860–921.
48. Waterston,R.H., Lindblad-Toh,K., Birney,E., Rogers,J., Abril,J.F., Agarwal,P., Agarwala,R., Ainscough,R., Alexandersson,M. *et al.* (2002) Initial sequencing and comparative analysis of the mouse genome. *Nature*, **420**, 520–562.
49. Houbaviy,H.B., Murray,M.F. and Sharp,P.A. (2003) Embryonic stem cell-specific MicroRNAs. *Dev. Cell*, **5**, 351–358.
50. Kasashima,K., Nakamura,Y. and Kozu,T. (2004) Altered expression profiles of microRNAs during TPA-induced differentiation of HL-60 cells. *Biochem. Biophys. Res. Commun.*, **322**, 403–410.
51. Lewis,B.P., Burge,C.B. and Bartel,D.P. (2005) Conserved seed pairing, often flanked by adenosines, indicates that thousands of human genes are microRNA targets. *Cell*, **120**, 15–20.
52. Liu,J.D., Valencia-Sanchez,M.A., Hannon,G.J. and Parker,R. (2005) MicroRNA-dependent localization of targeted mRNAs to mammalian P-bodies. *Nat. Cell Biol.*, **7**, 719–723.
53. Maniataki,E. and Mourelatos,Z. (2005) A human, ATP-independent, RISC assembly machine fueled by pre-miRNA. *Genes Dev.*, **19**, 2979–2990.
54. Tang,G. (2005) siRNA and miRNA: an insight into RISCs. *Trends Biochem. Sci.*, **30**, 106–114.